epl A Letters Journal Exploring the Frontiers of Physics

August 2012

EPL, **99** (2012) 48003
doi: 10.1209/0295-5075/99/48003

www.epljournal.org

Experimental link of coarsening rate and volume distribution in dry foam

J. Lambert[1], F. Graner[2,3], R. Delannay[1] and I. Cantat[1(a)]

[1] *IPR UMR 6251, Université Rennes I - F-35042 Rennes Cedex, France, EU*
[2] *"Polarité, Division et Morphogenèse", Laboratoire de Génétique et Biologie du Développement, Institut Curie 26 rue d'Ulm, F-75248 Paris Cedex 05, France, EU*
[3] *Matière et Systèmes Complexes, Université Paris Diderot, CNRS UMR 7057 10 rue Alice Domon et Léonie Duquet, F-75205 Paris Cedex 13, France, EU*

received 10 May 2012; accepted in final form 17 July 2012
published online 23 August 2012

PACS 82.70.Rr – Aerosols and foams
PACS 83.80.Iz – Emulsions and foams

Abstract – In dry foam, we investigate the link between coarsening rate and bubble distribution. Revisiting Mullins' predictions (Mullins W. W., *J. Appl. Phys.*, **59** (1986) 1341), we predict, without any phenomenological assumption, that the volume distribution behaves as $v^{(2-D)/D}$ (where D is the dimension of space) in the limit of small volumes. This is in agreement with recent experimental results. In the self-similar growth regime, we validate experimentally a relation between the bubbles' growth rates and their size distribution. In 2D, we discuss the relation between the areas distribution and the correlation between edge numbers and bubble area.

Introduction. – Coarsening in cellular systems like liquid foams and grains in crystals has been studied for long both experimentally and theoretically. In liquid foams, for example, the coarsening is due to the gas flow between neighboring bubbles induced by their pressure difference [1,2]. The equations governing the dynamics of those systems has been investigated by Mullins who focused on the late-stage dynamics assuming the existence of a Self-Similar Growth Regime (SSGR) of the volume distribution at different times. This assumption led Mullins to a now classical prediction on the average bubble size time evolution [3]:

$$\frac{\mathrm{d}\bar{v}}{\mathrm{d}t} = C\bar{v}^{\alpha}, \tag{1}$$

where $\bar{v}$ is the average bubble volume in 3D and the average bubble area in 2D, C is a constant that depends on the physico-chemistry of the foam and α is a constant that depends on the dimension of the space D: $\alpha = (D-2)/D$, so $\alpha_{3D} = 1/3$ and $\alpha_{2D} = 0$. A direct consequence of eq. (1) is that $\bar{R}(t)^2 - \bar{R}(0)^2 \propto t$, with $\bar{R} \sim \bar{v}^{1/D}$ the average bubble radius.

Mullins also established that the growth rate of individual bubbles can be deduced from the bubble size distribution (the exact relation is given below eq. (10)), which had been successfully tested by Streitenberger *et al.* using 3D numerical simulations [4]. In this paper, we show a first experimental proof of this relation for the case of low-liquid fraction 3D foams. In addition, we establish new consequences of the general theory developed by Mullins. We predict a power law behavior at small volumes for the 3D bubble size distribution and test this prediction experimentally. In the last part of the paper, we focus on 2D foam. A linear relation between the number of edges averaged over the set of bubbles sharing the same area and the bubble area is often assumed in the literature, which implies an exponential decay of the area distribution in SSGR [5]. It has been recently proposed that this average number of edges varies as the bubble area to the power 1/2 [6], thus leading to another area distribution [4]. We compare both area distributions to experimental data, and get a better agreement with the last one.

Growth rate. – In a dry foam, the bubbles' shapes strongly depart from the spherical shape. In the limit of vanishing liquid fraction, the bubbles are polyhedra with slightly curved faces and well-defined edges. The curvature of the faces and the pressure in each bubble are related to each other through the Laplace law. The pressure difference between two neighboring bubbles induces a slow gas flux governed by Fick's law, and the volume evolution

(a) E-mail: isabelle.cantat@univ-rennes1.fr

is given by [1,2]

$$\frac{\mathrm{d}v}{\mathrm{d}t} = D_{eff} \int K \mathrm{d}s, \tag{2}$$

where K is the bubble mean curvature; v and $\mathrm{d}s$ are, respectively, the bubble volume and an element of its surface in 3D, and the bubble area and an element of its perimeter in 2D; D_{eff} is an effective diffusion coefficient depending on the physico-chemistry of the foam and on the films' thickness. This last parameter is constant in time for dry foams.

The growth rate of a bubble is defined as $\mathcal{G} = v^{-\alpha}\mathrm{d}v/\mathrm{d}t$ and can be expressed as

$$\mathcal{G} = D_{eff} \int \frac{K}{v^{\alpha}} \mathrm{d}s. \tag{3}$$

As K scales as $v^{-1/D}$, $\mathrm{d}s$ as $v^{(D-1)/D}$ and $v^{-\alpha}$ as $v^{-(D-2)/D}$, it follows that the integral does not depend on v, meaning that $\mathcal{G}$ is not modified by a homothetic transformation of the bubble and only depends on its shape [7]. In 2D, the von Neumann law states that $\mathcal{G}$ only depends on the number of neighbors F [8]:

$$\mathcal{G}^{2D} = D_{eff}^{2D}(F-6). \tag{4}$$

The extension of this expression in 3D involves more complex geometrical quantities, and not only the faces number [9]. However, statistically, $\mathcal{G}$ increases with the number of faces (see [10–13] and the review [14]). As the bubble volume, compared to the average bubble volume in the foam, and the number of faces are strongly correlated, $\mathcal{G}$ also increases with v statistically.

Model: small volume limit of the volume distribution. – The distribution of $\mathcal{G}$ determines the time evolution of the bubble size distribution as well as the evolution of the bubble number. We consider $N(t)$ bubbles coarsening in a closed volume V, and $P(v,t)$ the volume distribution at time t, normalized to unity. Defining $\mathcal{G}_v$ as the growth rate averaged over the set of bubbles sharing the same volume, we get

$$\frac{1}{N}\frac{\mathrm{d}N}{\mathrm{d}t} = \lim_{v\to 0} \mathcal{G}_v(v) v^{\alpha} P(v,t). \tag{5}$$

This relation, established by Mullins (eq. (6) in ref. [3], see A) in the appendix) requires a few comments. First, this relation only makes sense if the foam sample is large enough so that its various properties can have a continuous representation. More precisely, the time scale of the observation must be large enough to consider the bubble number as a continuous function of time, and the typical length scale of the description must be large enough for the limit of vanishing volume to be defined. Second, even in a very large foam, the smallest bubble volume may be limited by the finite volume v_v of the vertices in which the bubbles eventually dissolve, so we only discuss here the limit of very dry foams. Finally, let us underline the fact that eq. (5) does not assume that the SSGR is reached.

As the bubble size decreases, its number of faces decreases and, on average, its internal pressure increases to a much higher pressure than its neighbors. This explains why $\mathcal{G}$ reaches a finite and strictly negative value in the limit of small volumes. So we define $\mathcal{G}_0$ as the limit of $\mathcal{G}_v$ at vanishing volumes and obtain

$$\frac{1}{N}\frac{\mathrm{d}N}{\mathrm{d}t} = \mathcal{G}_0 \lim_{v\to 0} v^{\alpha} P(v,t). \tag{6}$$

For a foam in which the coarsening process is already established (but possibly still in its transient stage), the bubble number regularly decreases ($\mathrm{d}N/\mathrm{d}t < 0$). This imposes the asymptotic behavior of the volume distribution at small scale.

In 3D, $\alpha = 1/3$ and $\mathrm{d}N/\mathrm{d}t \neq 0$ only if $P(v,t)$ diverges in 0 as $v^{-1/3}$:

$$P(v,t) \sim A v^{-1/3} \tag{7}$$

with $A = \mathcal{G}_0^{-1}\frac{1}{N}\frac{\mathrm{d}N}{\mathrm{d}t}$. This consequence of Mullins' theory is in good agreement with our experiments as will be shown hereafter. The theoretical prediction of $\mathcal{G}_0$ would require the knowledge of the foam dynamics at small volumes, which is not yet described. However, it may be assumed that tetrahedra dominate the small size bubble shape distribution. In this case, the high internal pressure enforces equality of the 4 faces' curvatures and thus a symmetrical shape for the tetrahedron. This symmetry is more and more precisely achieved as the volume decreases and the pressure increases. Under this assumption, the value of $\mathcal{G}_0$ can be calculated from eq. (3) if the prefactor D_{eff} is known: $\mathcal{G}_0 = -3.97\, D_{eff}$ [14]. The same asymptotic bubble size distribution is found for bubbly liquids, governed by Oswald ripening, for the interface limited case [15]. This comes from the fact that, also in that case, $\mathcal{G}$ reaches a finite limit at small volume. However, the full distribution is significatively different from what is found for dry foams.

In 2D, $\alpha = 0$, leading to the relation

$$\lim_{v\to 0} P(v,t) = \frac{1}{N\mathcal{G}_0}\frac{\mathrm{d}N}{\mathrm{d}t} \tag{8}$$

which simply states that $P(v,t)$ reaches a finite value at small volume. If $\mathcal{G}_0$ is given by the growth rate of 3-faces bubbles, then $\mathcal{G}_0 = -3D_{eff}^{2D}$.

Note that using the bubble radius R instead of the volume v as variable leads to the same relation in all dimensions: $P(R) \sim R$ at small R.

Model: self-similar growth regime. – In the SSGR, all scale-independent quantities become statistically time independent. The normalized distribution of reduced volume $x = v/\bar{v}(t)$, with $\bar{v}(t) = V/N(t)$ the average volume, is defined as $\hat{P}(x) = \bar{v}(t)P(v,t)$ and does not depend on time. The distribution $\hat{P}(x)$ is likely to be universal [16] and can thus be considered as a

well-defined continuous function, independent of the initial preparation of the foam.

In the SSGR, the time evolution of $P(v,t)$ is entirely governed by the variation of the bubble number $\mathrm{d}N/\mathrm{d}t$, or equivalently, by the variation of the average volume $\bar{v}(t) = V/N(t)$. This becomes explicit by using the reduced distribution which is, by definition, invariant during the SSGR:

$$P(v,t) = \frac{1}{\bar{v}(t)} \hat{P}(v/\bar{v}(t)). \qquad (9)$$

On the one hand, we can predict $P(v, t+\mathrm{d}t)$ from eq. (9) if we know $P(v,t)$, $\bar{v}(t)$ and $\bar{v}(t+\mathrm{d}t)$. On the other hand, by definition of the growth rate $\mathcal{G}$, we can deduce $P(v, t+\mathrm{d}t)$ from $P(v,t)$ and the distribution of $\mathcal{G}$ at any given time.

Both predictions of $P(v, t+\mathrm{d}t)$ must lead to the same values, which simply implies that, in the SSGR, the bubble size distribution, the time evolution of the bubble number and the growth rates distribution are not independent. The exact relation between these three quantities has been established by Mullins in 1986 [3]. More precisely, Mullins gave the prediction of the growth rate averaged over the set of bubble of same volume, $\mathcal{G}_v$, as a function of the bubble size distribution, $P(v)$, and of the bubble number variation:

$$\mathcal{G}_v(v) = \frac{1}{N}\frac{\mathrm{d}N}{\mathrm{d}t}\frac{1}{P(v)v^\alpha}\left(\int_v^\infty P(v)\mathrm{d}v - vP(v)\right). \qquad (10)$$

This relation is the eq. (13) in [3], expressed as a function of the variables $\mathcal{G}_v$ and $P(v)$ for which we recently provided 3D experimental measurement for foams, respectively, in [17] and [16] (the transformation is given in B) in the appendix).

Comparison with 3D experimental results in SSGR. – Experimental data have been obtained with a dry dishwashing liquid foam, 190 min after its making (same data as in [16], fig. 3). At this time of its evolution, the relative variation of the bubble number is $\frac{1}{N}\frac{\mathrm{d}N}{\mathrm{d}t} = -1.5\cdot10^{-4}\,\mathrm{s}^{-1}$ and the liquid fraction is $2.0\% \pm 0.2$. The volume distribution is plotted in fig. 1. Fixing the exponent at $-1/3$, we fit $P(v)$ as $A\,v^{-1/3}$ with $A = 13.5$ mm^{-2}. Given the value of $\frac{1}{N}\frac{\mathrm{d}N}{\mathrm{d}t}$, this corresponds to $\mathcal{G}_0 = -11.1\,\mu\mathrm{m}^2\cdot\mathrm{s}^{-1}$, in good agreement with the value found experimentally (see fig. 2). At large volume, an exponential decay is found. A Gamma distribution $\Gamma(v) = (v/v_0)^{s-1}e^{-v/v_0}/(v_0\Gamma(s))$ is classically used to fit grain volume distributions, with the shape exponent s as adjustable parameter [18]. The fact that the distribution must vary like $v^{-1/3}$ at small volumes imposes the value of the shape exponent $s = 2/3$. The agreement with the bubble volume distribution is good, as shown in fig. 1.

From the experimental bubble size distribution shown in fig. 1, we compute $\mathcal{G}_v^{cal}(v)$ using eq. (10). $\mathcal{G}_v^{cal}(v)$ is plotted in fig. 2 and compared with the direct measurement of $\mathcal{G}_v^{exp}(v)$ based on the bubble tracking between times 188 min and 194 min on the same foam. The image processing method has already been used for a slightly wetter foam in [17] where the different steps of the analysis are discussed. The difference between $\mathcal{G}_v^{mes}$ and $\mathcal{G}_v^{cal}$ is within the statistical fluctuations, without any adjustable parameter. Equation (10) is thus experimentally verified. One may simply notice a small discrepancy at very small volumes: $\mathcal{G}_v^{mes}$ is larger than expected at small volumes. This is very likely due to the non-negligible size of the meniscus for those volumes. This reduces the accessible area for gas transfer and leads to a smaller $\mathcal{G}_v^{mes}$ in absolute value [17].

A simple analytical prediction $\mathcal{G}_v^{expo}$ is obtained for an exponential volume distribution:

$$\mathcal{G}_v^{expo} = \frac{1}{N}\frac{\mathrm{d}N}{\mathrm{d}t}\frac{\bar{v}-v}{v^{1/3}}. \qquad (11)$$

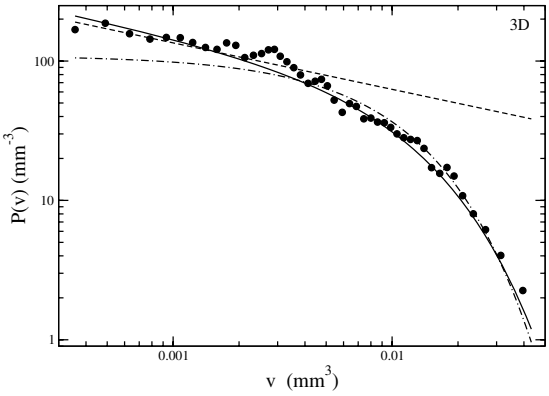

Fig. 1: Normalized volume distribution in self-similar growth regime. The full line is the Γ distribution $P(v) = (v/v_\Gamma)^{-1/3}e^{-v/v_\Gamma}/(\Gamma(2/3)v_\Gamma)$ with $v_\Gamma = 0.011\,\mathrm{mm}^3$; the dot-dashed line is the exponential law $P(v) = (1/v_0)\,e^{-v/v_0}$, with $v_0 = 0.00913\,\mathrm{mm}^3$; the dashed line is the power law $P(v) = 13.5\,v^{-1/3}$.

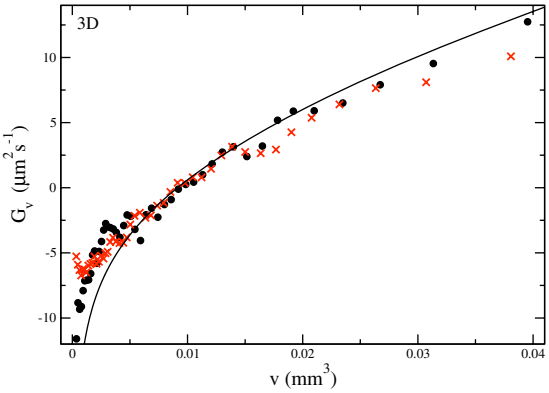

Fig. 2: (Colour on-line) Bubble growth rate in 3D. The individual growth rate in a 3D dry foam during the SSGR is averaged over a set of bubbles having the same volume. ×: $\mathcal{G}_v^{mes}$ directly measured from the volume variation of bubbles followed between $t = 188$ min and $t = 194$ min. Each point represents an average over 100 bubbles of similar volume. •: $\mathcal{G}_v^{cal}$ obtained from eq. (10) with the distribution plotted in fig. 1 and $\frac{1}{N}\frac{\mathrm{d}N}{\mathrm{d}t} = 1.5\cdot10^{-4}\,\mathrm{s}^{-1}$. Full line: $\mathcal{G}_v^{exp}$ given by eq. (11), based on the assumption of an exponential volume distribution.

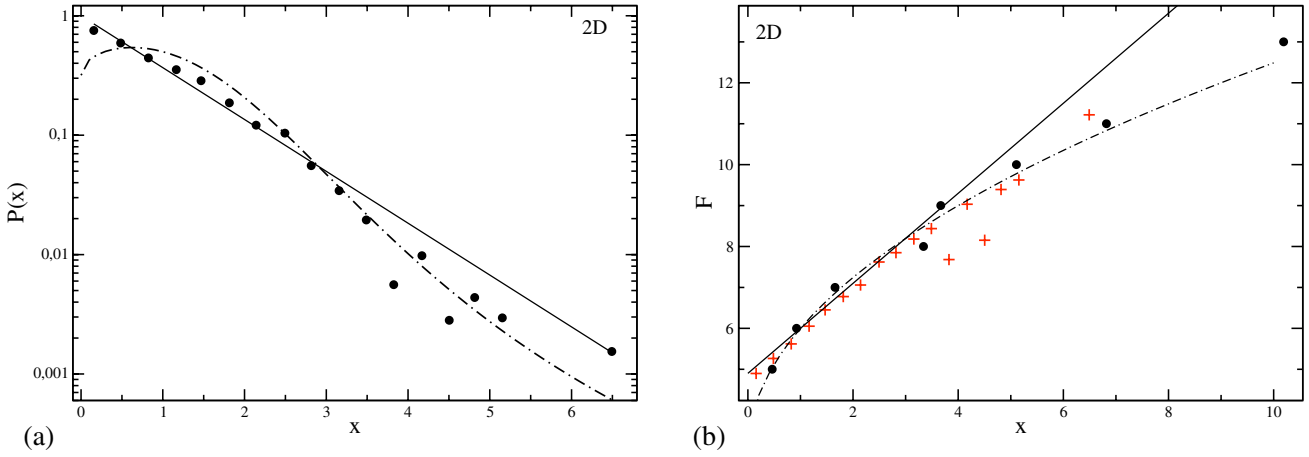

Fig. 3: (Colour on-line) Self-similar growth regime in 2D. (a) •: bubble area distribution (fig. 5.22 in ref. [19]). The full line is the exponential distribution and the dash-dotted line the distribution given by eq. (18). (b) $+$: F plotted as a function of the experimental value of $x = \langle a \rangle_F / \bar{a}$ (from fig. 3.17a in ref. [19]). The average area is adjusted. •: F obtained from eq. (14), with the experimental distribution (a) and the adjustable prefactor $C/D_{eff}^{2D} = 0.95$. The full line and the dash-dotted line correspond, respectively, to the relations between faces number and average area given by eq. (15) and eq. (17).

$\mathcal{G}_v^{expo}$ roughly fits the experimental distribution, with an underestimation of the smallest volumes (see fig. 1). The agreement between $\mathcal{G}_v^{mes}$ and $\mathcal{G}_v^{expo}$ is satisfying, and eq. (11) is thus a very convenient analytical prediction for the growth rate in SSGR (see fig. 2).

2D case and correlation between area and edges number. – In two dimensions, the exponent α is zero and the bubble area a replaces the volume v. Equation (10) becomes

$$\mathcal{G}_v^{2D}(a) = \frac{1}{N}\frac{\mathrm{d}N}{\mathrm{d}t}\frac{1}{P(a)}\left(\int_a^\infty P(a)\mathrm{d}a - aP(a)\right) \qquad (12)$$

or, using the reduced variable $x = a/\bar{a}$ and the constant $C = \mathrm{d}\bar{a}/\mathrm{d}t$

$$\mathcal{G}_v(x) = -C\left(\frac{1}{\hat{P}(x)}\int_x^\infty \hat{P}(x)\mathrm{d}x - x\right). \qquad (13)$$

Furthermore the growth rate in 2D is an exact function of F, the face number of the bubble (see eq. (4)). Averaging over the set of bubbles having the same area we get, from eq. (13) (see also [6], eq. (49))

$$\langle F \rangle_a = 6 + \frac{C}{D_{eff}^{2D}}\left(x - \frac{1}{\hat{P}(x)}\int_x^\infty \hat{P}(x')\mathrm{d}x'\right). \qquad (14)$$

Experimental data have been obtained by Pignol [19] on 2D foam in SSGR. We plot the area distribution of a coarsening 2D foam in SSGR in fig. 3(a). The quantity that is usually plotted to characterize the foam structure is $\langle a \rangle_F$ (see, *e.g.*, [19]). Despite the fact that this average may differ from $\langle F \rangle_a$, we compare $\langle a \rangle_F$ to the predictions obtained with eq. (14) in fig. 3(b). As neither the kinetic factors C/D_{eff}^{2D} nor the average area are available, these quantities are taken as adjustable parameters.

For an exponential area distribution, eq. (14) becomes [5]

$$\langle F \rangle_a = 6 + \frac{C}{D_{eff}^{2D}}(x-1). \qquad (15)$$

In the SSGR, there is thus an equivalence between a linear behavior of the average edge number $\langle F \rangle_a$ as a function the area and an exponential area distribution. Both laws are represented in fig. 3 using full lines and compared to experimental data.

Recently, the relation

$$\langle F \rangle_a = 3(1 + \sqrt{a}/\langle\sqrt{a}\rangle) \qquad (16)$$

has been predicted theoretically [6], thus questioning the exponential behavior of the area distribution in coarsening foams.

The general expression of the area distribution in a foam as a function of an arbitrary growth rate has been derived in [4]. We provide below the explicit expression for the distribution corresponding to the growth rate of interest here, obtained by approximating eq. (16) by

$$\langle F \rangle_a = 3(1 + \sqrt{x}). \qquad (17)$$

Inverting eq. (14) with $C/D_{eff}^{2D} = 0.95$ (see fig. 3(a), dash-dotted line) leads to the semi-analytical area distribution:

$$\hat{P}(x) = \hat{P}(0)\frac{\exp[-1.94 + 3.87\arctan(1.94 - 1.23\sqrt{x})]}{(3.16 - 3.16\sqrt{x} + x)^2}. \qquad (18)$$

This distribution provides a better agreement with experimental data than an exponential decay for large bubbles. For small bubbles this law is less satisfying.

Nevertheless, the experimental distribution in SSGR shown in [20] (fig. 6) differs significantly from fig. 3 for small bubbles and is in qualitative agreement with the prediction (eq. (18)).

Conclusion. – In this paper we highlighted the strong relation between the bubble's growth rates and their size distribution in the self-similar growth regime. One can be deduced from the other and the other way around. This opens new perspectives both in the theoretical and experimental fields. On the experimental ground, $P(v)$ is far easier to measure than $\mathcal{G}_v$ since the latter quantity requires the correlation of two successive images. In contrast one theoretical challenge is to predict $P(v)$ in the SSGR. Most attempts to derive $P(v)$ rely on assumptions like maximum entropy [21]. However, another way to proceed could be based on a local estimation of $\mathcal{G}_v$. This way has been less investigated despite many efforts to predict $\mathcal{G}$ [9–14] and might be revealed as productive.

Appendix

Hereafter, as in Mullins' paper, $f(v,\dot{v},t)$ is the density of bubble of volume v and volume variation $\dot{v}=\mathrm{d}v/\mathrm{d}t$, with $\int f(v,\dot{v},t)\mathrm{d}v\mathrm{d}\dot{v}=1$ and $\int f(v,\dot{v},t)\mathrm{d}\dot{v}=P(v)$; $\rho(v,\dot{v},t)=Nf(v,\dot{v},t)$; $\phi(x,y)$ is the reduced density (normalized to unity) defined by $\phi(x,y)=\bar{v}^{(1+\alpha)}f(v,\dot{v},t)$, with $x=v/\bar{v}$ and $y=\dot{v}/\bar{v}^{\alpha}$, so that $\phi(x,y)$ does not depend on time in the SSGR; finally, $\tilde{\phi}(x)=\int_{-\infty}^{\infty}\phi(x,y)\mathrm{d}y=\bar{v}P(v)$.

A) Transformation of eq. (6) from [3] into the relation (5):

$$\frac{\mathrm{d}N}{\mathrm{d}t}=\lim_{v_0\to 0}\int_{-\infty}^{0}\mathrm{d}\dot{v}\dot{v}\rho(v_0,\dot{v},t) \tag{A.1}$$

$$=N\lim_{v_0\to 0}P(v_0)\langle\dot{v}\rangle_{v=v_0} \tag{A.2}$$

$$=\lim_{v_0\to 0}NP(v_0)\mathcal{G}_v(v_0)v_0^{-1/3}. \tag{A.3}$$

B) Transformation of eq. (13a) from [3] into the relation (10). Equation (13a) is

$$-C\frac{\mathrm{d}}{\mathrm{d}x}\left(x\int_x^{\infty}\tilde{\phi}(x')\mathrm{d}x'\right)=\int_{-\infty}^{\infty}\phi(x,y)y\mathrm{d}y. \tag{A.4}$$

We get for the right-hand side

$$\int_{-\infty}^{\infty}\phi(x,y)y\mathrm{d}y=\int_{-\infty}^{\infty}f(v,\dot{v},t)\bar{v}^{(1+\alpha)}\frac{\dot{v}}{\bar{v}^{\alpha}}\frac{\mathrm{d}\dot{v}}{\bar{v}^{\alpha}} \tag{A.5}$$

$$=\bar{v}^{(1-\alpha)}v^{\alpha}\int_{-\infty}^{\infty}f(v,\dot{v},t)v^{-\alpha}\dot{v}\mathrm{d}\dot{v} \tag{A.6}$$

$$=\bar{v}^{(1-\alpha)}v^{\alpha}P(v)\mathcal{G}_v \tag{A.7}$$

and for the left-hand side, using eq. (1)

$$-C\frac{\mathrm{d}}{\mathrm{d}x}\left(x\int_x^{\infty}\tilde{\phi}(x')\mathrm{d}x'\right)=-C\left(\int_x^{\infty}\tilde{\phi}(x')\mathrm{d}x'-x\tilde{\phi}(x)\right) \tag{A.8}$$

$$=-\frac{\mathrm{d}\bar{v}}{\mathrm{d}t}\bar{v}^{-\alpha}\left(\int_v^{\infty}P(v)\mathrm{d}v-vP(v)\right). \tag{A.9}$$

Finally

$$\bar{v}^{(1-\alpha)}v^{\alpha}P(v)\mathcal{G}_v=-\frac{\mathrm{d}\bar{v}}{\mathrm{d}t}\bar{v}^{-\alpha}\left(\int_v^{\infty}P(v)dv-vP(v)\right), \tag{A.10}$$

$$\mathcal{G}_v=\frac{1}{N}\frac{\mathrm{d}N}{\mathrm{d}t}\frac{1}{P(v)v^{\alpha}}\left(\int_v^{\infty}P(v)\mathrm{d}v-vP(v)\right). \tag{A.11}$$

REFERENCES

[1] Weaire D. and Hutzler S., *The Physics of Foams* (Oxford University Press, Oxford) 2000.
[2] Cantat I. *et al.*, *Les mousses. Structure et dynamique* (Belin, Paris) 2010.
[3] Mullins W. W., *J. Appl. Phys.*, **59** (1986) 1341.
[4] Streitenberger P. and Zöllner D., *Scr. Mater.*, **55** (2006) 461.
[5] Flyvbjerg H., *Phys. Rev. E*, **47** (1993) 4037.
[6] Durand M. *et al.*, *Phys. Rev. Lett.*, **107** (2011) 168304.
[7] Glazier J., *Phys. Rev. Lett.*, **70** (1993) 2170.
[8] von Neumann J., in *Metal Interfaces* (American Society for Metals, Cleveland) 1952, pp. 108–110.
[9] MacPherson R. and Srolovitz D., *Nature*, **446** (2007) 1053.
[10] Mullins W. W., *Acta Metall.*, **37** (1989) 2979.
[11] Hilgenfeldt S., Kraynik A. M., Koehler S. A. and Stone H. A., *Phys. Rev. Lett.*, **86** (2685) 2001.
[12] Hilgenfeldt S., Kraynik A. M., Reinelt D. A. and Sullivan J. M., *Europhys. Lett.*, **67** (2004) 484.
[13] Wang H., Liu G. Q., Song X. Y. and Luan J. H., *EPL*, **96** (2011) 38003.
[14] Jurine S., Cox S. and Graner F., *Colloids Surf. A*, **263** (2005) 18.
[15] Markworth A. J., *Metallography*, **3** (1970) 197.
[16] Lambert J. *et al.*, *Phys. Rev. Lett.*, **104** (2010) 248304.
[17] Lambert J. *et al.*, *Phys. Rev. Lett.*, **99** (2007) 058304.
[18] Vaz M. F. and Fortes M., *Scr. Metall.*, **22** (1988) 35.
[19] Pignol V., *Évolution et caractérisation de structures cellulaires bidimensionnelles expérimentales, en particulier les mousses de savons, et simulées*, PhD Thesis, INPL, 1996, `http://tel.archives-ouvertes.fr/tel-00717860`.
[20] Duplat J., Bossa B. and Villermaux E., *J. Fluid Mech.*, **673** (2011) 147.
[21] Thomas G. L., de Almeida R. M. C. and Graner F., *Phys. Rev. E*, **74** (2006) 021407.